J|A|C|S
COMMUNICATIONS

Published on Web 12/13/2006

Shape Selectivity in the Assembly of Lithographically Designed Colloidal Particles

Stéphane Badaire, Cécile Cottin-Bizonne,† Joseph W. Woody, Allen Yang, and Abraham D. Stroock*

School of Chemical and Biomolecular Engineering, Cornell University, Ithaca, New York 14853

Received October 20, 2006; E-mail: ads10@cornell.edu

There is an outstanding need for methods with which to form complex, three-dimensional structures on the colloidal scale (10 nm to 10 μm). Such methods would be valuable for the development of photonics,[1a] high-density memory[1b] and electronics,[1c] and micromechanical devices.[1d] An attractive approach to this challenge is to exploit the concepts of chemical thermodynamics to form structure from colloidal particles.[2] This approach, based on self-assembly, requires the development of a diversity of building blocks, selective and directional interactions, and methods of processing. In this communication, we describe the development of a self-assembling colloidal system based on photolithographic fabrication of particles and tailored electrostatic and depletion interactions.

Significant progress has been made in recent years toward the controlled assembly of colloidal particles. A broad array of structures has been achieved with micrometer-scale[1a,3] and nanometer-scale[4] particles via assembly far from equilibrium (e.g., evaporation of solvent from the dispersion). While these methods have proved versatile, they often leave the mechanism of assembly obscure. Bibette[5] in 1991 pioneered the use of the geometry dependence of the depletion interaction[6]—osmotic-based attractive force between surfaces in the presence of a nonadsorbing solute—to drive phase separation near equilibrium. Over the past decade, others have exploited this phenomenon to generate structure via geometry-dependent interactions of colloids with surfaces[7] or colloids with colloids.[8] This strategy, which is based on near-equilibrium behavior, is amenable to rational design of selective "bonds" on the colloidal scale, but its use has been hindered by the lack of colloids with well-defined size and nonspherical shape and by an incomplete accounting of the colloidal interactions at play. Here, we have advanced the use of this strategy with the demonstration of (i) a photolithographic route to monodisperse, well-defined nonspherical colloids and (ii) the induction of tunable, shape-selective interactions and extended order based on depletion, electrostatic, and van der Waals (vdW) forces.

Figure 1A illustrates the photolithographic procedure by which we form cylindrical particles directly in an epoxy-based negative photoresist, SU-8 (2002 and 2000.5 series). The key aspects of the process include the following: (1) Spin coating of the resist on top of a sacrificial layer on a silicon substrate. This step controls the height of the particles, h; we have achieved 300 nm $< h <$ 3 μm. (2) Exposure of the resist to ultraviolet light (i-line) through a photomask with round holes. This step defines the diameter, d, of the particles; we have achieved 0.8 μm $< d <$ 8 μm. (3) Development of the photopatterned layer of resist, release of the particles via dissolution of the sacrificial layer, washing, and resuspension in a buffered aqueous solution of Tergitol NP40, a non-ionic surfactant ([NP40] = 75 μM (0.015$_{wt\%}$) < critical micelle concentration = 120 μM; buffer = 1 mM Tris-HCl, pH = 8.3 at 23 °C); the NP40 eliminated adhesion of the particles to plastic containers and stabilized them against irreversible aggregation. We will refer to this buffer as our standard solution. This route generated ~10^9 colloidal particles per 100 mm wafer. A detailed experimental procedure, as well as the characterization (size distribution, ζ-potential, and roughness) of the particles of aspect ratio h:d = 1:1 (Figure 1B) and h:d ~ 1:3 (Figure 1C) used in this study, is presented in Supporting Information.

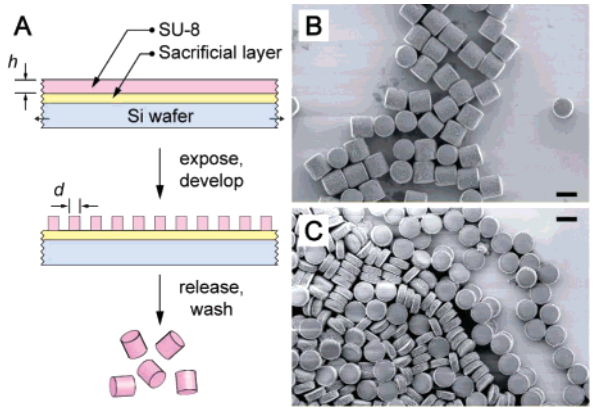

Figure 1. Fabrication of colloids. (A) Schematic diagram of formation of cylindrical particles in an epoxy-based negative photoresist (SU-8) via projection photolithography. (B and C) Scanning electron micrographs (SEMs) of SU-8 particles produced by this process and redeposited on a silicon wafer from water. Particle dimensions: $h = 1.19 \pm 0.08$ μm and $d = 1.20 \pm 0.08$ μm in (B); $h = 415 \pm 46$ nm and $d = 1.15 \pm 0.07$ μm in (C).

We employed these particles to explore the use of depletion and DLVO[6] (vdW + electrostatics) forces to generate shape selectivity. The distinction in shape—both global curvature and roughness (12 nm rms roughness on sidewalls; 4 nm rms on flat ends)—of the sidewalls relative to the ends of these particles implies distinct steric constraints on their interactions when oriented end-to-end, end-to-side, and side-to-side: the smooth, flat ends will be able to form closer, more extended contact than the rough, rounded sides. An evaluation of the electrostatic, van der Waals, and depletion interactions for smooth cylindrical particles predicts orientationally selective interactions: end-to-end interactions will be favored over end-to-side and side-to-side (see Supporting Information).

To explore this prediction experimentally, we observed the evolution of dispersions of cylinders in our standard solution at a constant particle concentration: $C_n = 6 \times 10^6$ particles/μL, corresponding to a particle volume fraction, $\Phi_c \sim 0.8\%$, in the case of cylinders of aspect ratio 1:1, and $\Phi_c \sim 0.3\%$ in the case of cylinders of aspect ratio 1:3. We adjusted the depletion interactions between the particles with the addition of dextran (M_w = 172 000 g/mol, $M_w/M_n = 2.16$, $R_g = 12$ nm[9]); we have verified that dextran does not adsorb to the surface of these particles (see Supporting Information). We adjusted the electrostatic interactions by varying the ionic strength with the addition of sodium chloride. We enclosed

† Present address: Laboratoire de Physique de la Matière Condensée et Nanostructures, Université Lyon 1, CNRS, UMR 5586, 69622 Villeurbanne, France.

10.1021/ja067527h CCC: $37.00 © 2007 American Chemical Society

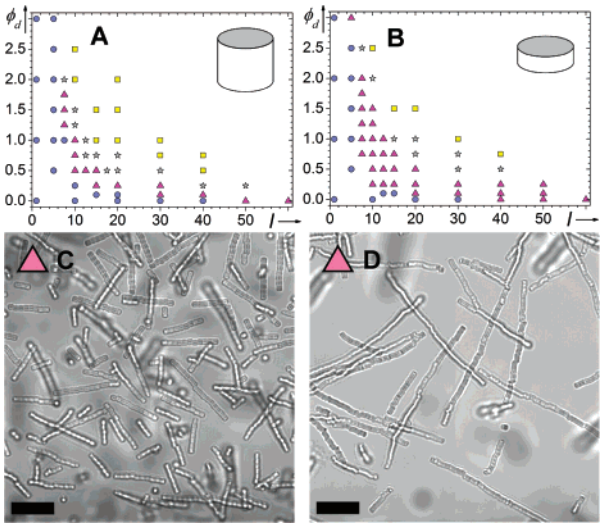

Figure 2. Selective interactions tuned with shape, electrostatics, and depletion. (A and B) Diagrams of the different states observed in dispersions of cylindrical particles of aspect ratio 1:1 (as in Figure 1B) (A) and aspect ratio 1:3 (as in Figure 1C) (B), at various ionic strengths, I [mM], and volume fractions of dextran, ϕ_d [%] in our standard solution. We identify four states: dispersed (blue circle), columnar (pink triangle), parallel and orthogonal aggregation (gray star), and isotropic aggregation (yellow square). (C and D) Optical micrographs of columnar states for 1:1 (C) and 1:3 (D) particles at $I = 10$ mM and $\phi_d = 0.75\%$. Scale bar $= 10\ \mu$m. See Supporting Information for a detailed description of the observed states.

dispersions in hermetically sealed glass capillaries with square cross-section (100 μm). Finally, we observed the dispersions by optical microscopy to identify characteristic structural states as a function of the ionic strength and the depletant volume fraction.

Figure 2 presents state diagrams for dispersions prepared with cylindrical particles of aspect ratio 1:1 (A) and 1:3 (B). States were assigned once dispersions showed no evolution over a 24-h period; most states stabilized within 24−48 h. Figure 2C and 2D presents micrographs of columnar states formed in dispersions of particles of aspect ratio 1:1 and 1:3 with $I = 10$ mM and $\phi_d = 0.75\%$ in both cases; Figures S7 and S8 present examples of all observed states. These results demonstrate the following important aspects of this new colloidal system: (i) Effective stabilization with NP40; the particles remain stable with respect to isotropic vdW aggregation up to the highest ionic strengths tested ($I = 200$ mM). (ii) Shape selectivity of electrostatic and vdW interactions. As seen in the state diagrams (Figure 2), we observed the formation of short columns (Figures S7 and S8) at elevated ionic strength with no depletant present (typically $I \geq 40$ mM). (iii) Increased shape selectivity in presence of depletion interactions (Figure 2C and 2D). We observed self-assembled columns with aspect ratio up to 60 (Figure S9); the formation of these structures implies that end-to-end interactions are several fold stronger than side-to-side interactions. Extended crystals also formed at higher volume fraction of the particles (Figure S6). (iv) Dependence of assembled structure on the shape of the individual particles. Comparing the behavior of the two types of particles, the shorter cylinders display higher selectivity for end-to-end assembly as seen by the broader columnar region in the state diagram (Figure 2B) and the increased number of particles per column; this observation is consistent with predictions (see Supporting Information). We also note that these assemblies form reversibly in the sense that the individual particles are still Brownian within the columns (movie "Columns.avi"; see Supporting Information); this characteristic implies that the structures are not stuck in deep kinetic traps, as is typical of assembly processes involving colloids.[1a] Finally, we note that these state diagrams are reproducible from one wafer to another.

In this communication, we have presented the rational design of a colloidal system that exhibits self-assembly of ordered, highly anisotropic structures. Our use of lithography to define the particles in a versatile organic material opens the possibility of adding distinct physical attributes, such as magnetism,[10a] electrical conductivity,[10b] and fluorescence,[10c] to the individual colloids. A generalization of this lithographic method will also give access to colloids in materials that are not accessible by synthetic paths, such as silicon and III−V compound semiconductors, and different shapes (see Figure S5 for examples). Our method of controlling the electrostatic and depletion interactions offers a powerful strategy for controlling the formation of order based on the structural motifs—curvature and roughness—presented on the surface of the particles. With the rapid growth in the diversity of nanoscale[11] and colloidal particles,[3a,12] these tools could help to overcome the outstanding challenges of 3D assembly on the micrometer and sub-micrometer scales, such as the formation of a direct diamond lattice.[13]

Acknowledgment. This work was supported by the Cornell Center for Materials Research (NSF-MRSEC, Grant DMR-0079992), the Cornell Center for Nanoscale Science (ECS 03-35765), the Cornell Nanobiotechnology Center (NSF-STC, No. ECS-9876771), the National Science Foundation (CTS-0529042), and the Camille and Henry Dreyfus Foundation. We are grateful to Prof. Fernando Escobedo for fruitful discussions.

Supporting Information Available: Experimental details and video of columnar state. This material is available free of charge via the Internet at http://pubs.acs.org.

References

(1) (a) Tetreault, N.; Miguez, H.; Ozin, G. A. *Adv. Mater.* **2004**, *16*, 1471−1476. (b) DeHon, A.; Goldstein, S. C.; Kuekes, P. J.; Lincoln, P. *IEEE Trans. Nanotechnol.* **2005**, *4*, 215−228. (c) Talapin, D. V.; Murray, C. B. *Science* **2005**, *310*, 86−89. (d) Bleil, S.; Marr, D. W. M.; Bechinger, C. *Appl. Phys. Lett.* **2006**, *88*, 263515.
(2) Xia, Y. N.; Gates, B.; Li, Z. Y. *Adv. Mater.* **2001**, *13*, 409−413.
(3) (a) Manoharan, V. N.; Elsesser, M. T.; Pine, D. J. *Science* **2003**, *301*, 483−487. (b) Yin, Y. D.; Lu, Y.; Xia, Y. N. *J. Am. Chem. Soc.* **2001**, *123*, 771−772. (c) Velikov, K. P.; Christova, C. G.; Dullens, R. P. A.; van Blaaderen, A. *Science* **2002**, *296*, 106−109.
(4) (a) Shevchenko, E. V.; Talapin, D. V.; Kotov, N. A.; O'Brien, S.; Murray, C. B. *Nature* **2006**, *439*, 55−59. (b) Kalsin, A. M.; Fialkowski, M.; Paszewski, M.; Smoukov, S. K.; Bishop, K. J. M.; Grzybowski, B. A. *Science* **2006**, *312*, 420−424.
(5) Bibette, J. *J. Colloid Interface Sci.* **1991**, *147*, 474−478.
(6) Hunter, R. J. *Foundations of Colloid Science*, 2nd ed.; Oxford University Press: Oxford, 2001.
(7) (a) Dinsmore, A. D.; Yodh, A. G.; Pine, D. J. *Nature* **1996**, *383*, 239−242. (b) Lin, K.; Crocker, J. C.; Prasad, V.; Schofield, A.; Weitz, D. A.; Lubensky, T. C.; Yodh, A. G. *Phys. Rev. Lett.* **2000**, *85*, 1770−1773.
(8) (a) Adams, M.; Dogic, Z.; Keller, S. L.; Fraden, S. *Nature* **1998**, *393*, 349−352. (b) Mason, T. G. *Phys. Rev. E* **2002**, *66*, 060402.
(9) Dogic, Z.; Purdy, K. R.; Grelet, E.; Adams, M.; Fraden, S. *Phys. Rev. E* **2004**, *69*, 051702.
(10) (a) Damean, N.; Parviz, B. A.; Lee, J. N.; Odom, T.; Whitesides, G. M. *J. Micro. Microeng.* **2005**, *15*, 29−34. (b) Jiguet, S.; Bertsch, A.; Hofmann, H.; Renaud, P. *17th IEEE International Conference on MEMS: Technical Digest* **2004**, 125−128. (c) Nilsson, D.; Balslev, S.; Gregersen, M.; Kristensen, A. *Appl. Opt.* **2005**, *44*, 4965−4971.
(11) Manna, L.; Milliron, D. J.; Meisel, A.; Scher, E. C.; Alivisatos, A. P. *Nat. Mater.* **2003**, *2*, 382−385.
(12) Liddell, C. M.; Summers, C. J. *Adv. Mater.* **2003**, *15*, 1715−1719.
(13) Maldovan, M.; Thomas, E. L. *Nat. Mater.* **2004**, *3*, 593−600.

JA067527H